Analysis, Simulation and Design of Series Resonant Converter for High Voltage Applications

Biju S. Nathan and V. Ramanarayanan
Department of Electrical Engineering,
Indian Institute of Science
Bangalore, INDIA 560 012
biju@ee.iisc.ernet.in, vram@ee.iisc.ernet.in

***Abstract*- Series Resonant Converters find application in high voltage power supplies where the large transformer parasitics have to be accounted for. This paper deals with the analysis, simulation and design of the Phase Modulated Series Resonant Converter. Steady state analysis for above resonant frequency operation is presented. Two modifications, one for extending the Zero Voltage Switching range and the other providing inherent short circuit protection are also introduced. Experimental results on a laboratory model are shown to verify the design procedure.**

I. INTRODUCTION

High voltage DC power supplies have a wide application range. Power levels in the kilowatt range are typical in applications like X-ray and radar. The load type may be static, pulsed, linear or non-linear. There are several challenging issues related to the design of such a power supply. Switched Mode topologies with high switching frequency are preferred in most cases because of the well known advantages offered by SMPC. Among the SMPC topologies, Series Resonant Converters (SRC) are preferred for high voltage, high power supplies [1]. The large parasitic leakage inductance of the high voltage transformer is effectively included into the resonant tank of the SRC. Switching losses and stress can be minimised as soft switching can be achieved. Higher switching frequencies are therefore possible bringing down the size of the converter and reducing generated EMI. On the output side, a simple capacitor filter is sufficient in case of the SRC; thus eliminating the need for costly and bulky high voltage filter inductors [1].

The classical SRC is a frequency controlled converter. The switching frequency is varied with respect to the resonant frequency to achieve the desired voltage gain. The variable switching frequency is a disadvantage. This paper deals with the Phase Modulated Series Resonant Converter (PM-SRC) which is a SRC operating at a fixed switching frequency and is duty ratio controlled. Steady state analysis of the PM-SRC operating above resonant frequency is carried out. Preferred operating modes are identified and design relations obtained. Numerical simulation is used to verify the analysis results. Experimental results on a laboratory prototype are used to confirm the design procedure. Two modified schemes to improve the performance of the PM-SRC are introduced. The first, to extend the Zero Voltage Switching (ZVS) range of the converter using an external inductive circuit and the other, an inherent short circuit protection method using resonant capacitor clamping technique.

II PM-SRC CIRCUIT DESCRIPTION

The PM-SRC (fig. 1) is also referred to as the phase shift controlled SRC or pulse width modulated SRC in the literature. It consists of a full bridge inverter feeding a series resonant tank. The tank current is rectified and filtered using a capacitive filter to produce the required dc voltage. High voltage is obtained using a step up transformer and voltage multiplier circuits (not shown).

Control is achieved through phase modulation [2]. Conduction of switches on the leading leg of the inverter $(S_1, \overline{S_1})$ is phase shifted with respect to the conduction of switches on the lagging leg $(\overline{S_2}, S_2)$ resulting in a quasi-square excitation voltage. Parasitic inductance of the transformer becomes part of the resonant inductance L_r. By including the resonant capacitor C_r and exciting the tank with a voltage waveform V_{in}, having frequency close to the tank resonant frequency, the effective impedance offered by the parasitic inductance to power flow is reduced. The circuit offers ZVS when operated above resonant frequency; this is preferred for a MOSFET based inverter.

III STEADY STATE ANALYSIS

A. Nomenclature

The resonant tank of the PM-SRC has a natural frequency determined by L_r and C_r (fig. 1).

f_s = switching frequency (freq. of exciting voltage)

f_r = resonant frequency $= \frac{1}{2\pi\sqrt{L_r C_r}}$ (1)

Relation between f_s and f_r is defined as $\gamma = \pi \frac{f_r}{f_s}$ (2)

If the width of the exciting voltage is of time T_{on}, duty ratio is defined as $D = \frac{T_{on}}{T_s/2}$ where $T_s = \frac{1}{f_s}$

The ratio of the output dc voltage to the supply voltage is the gain of the converter.

V_{dc} = supply voltage, V_o = output voltage

M = gain $= \frac{V_o}{V_{dc}}$ (3)

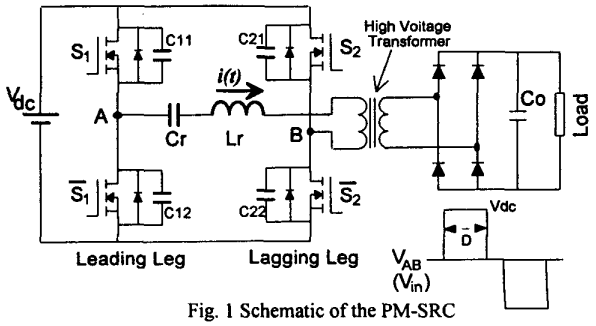

Fig. 1 Schematic of the PM-SRC

0-7803-5812-0/00/$10.00©2000IEEE

The parameter Z_c called the characteristic impedance of the tank is defined as

$$Z_c = \sqrt{\frac{L_r}{C_r}} \quad (4)$$

For a converter with a load resistance R_{load}, the load factor of the converter Q, is defined as

$$Q = \frac{Z_c}{R_{load}} \quad (5)$$

Instantaneous tank current and resonant capacitor voltage are represented by $i(t)$ and $v(t)$ respectively.

B. Normalised Variables

For simplifying the analysis and making the analysis results valid for a generic design method, all the parameters associated with the PM-SRC are normalised. Table I summarises the variables and the corresponding base values used in the analysis.

TABLE I BASE VARIABLES

Variable	Base
Voltage	Input DC Voltage, *Vdc*
Resistance	Z_c
Frequency	Resonant Frequency, ωr
Capacitance	$C_r = 1/Z_c\omega_r$
Inductance	$L_r = Z_c/\omega_r$

C. Assumptions

All components are assumed to be ideal. The output capacitive filter is large enough to approximate it as a constant voltage source under steady state. For simplifying the analysis, the transformer and voltage multipliers are not included. Effects of magnetising inductance and transformer parasitic capacitance are omitted. There is no power loss in the converter. V_{dc} is a constant through out the analysis.

D. Operating Modes and Equivalent Circuits

Under steady state, the PM-SRC switching above the resonant frequency has three modes of operation designated here as MODE 1, MODE 2 and MODE 3. Each mode further has sub-periods. The positive half sub-periods are shown in fig. 2. Each mode of operation consists of a sequence of sub-periods as indicated in table II.

For the steady state analysis, each mode is taken up individually and three consecutive sub-periods of that mode (constituting one half period) are analysed. The result can be extended to the full cycle of operation because of half wave symmetry. The analysis procedure followed here is similar to that in [3]. It involves deriving the circuit equations for each sub-period and relating the output voltage to the various circuit parameters namely Q, D and f_s/f_r. The implicit relation so obtained is solved iteratively to obtain the required design curves. The results from [3] cannot be extended to the PM-SRC because of the variable the duty ratio.

TABLE II SUB-PERIOD COMBINATIONS

Sub-Period Sequence	Operating Mode
C, A, B; C', A', B'	MODE 1 *
A, B, D; A', B', D'	MODE 2
A, B, E; A', B', E'	MODE 3

* *sub-period* B and B' do not exist for D = 1. A' indicates negative half of A

E. Analysis of MODE 1 *Operation*

Typical MODE 1 waveforms for $i(t)$ and $v(t)$ are plotted along with V_{in} and V_o in fig. 3. The operating cycle is defined here to start at time t=0 with *sub-period* C. Tank energy partly feeds the load and the rest is fed back to the source; thus $i(t)$ dies down. Because of resonance, $i(t)$ reverses direction at $t = T_1$ (*sub-period* A) resulting in the powering stage, where the source feeds the tank. In *sub-period* B ($t = T_2$) the resonant tank is clamped to zero voltage and $i(t)$ freewheels; the load draining away the tank energy. The output voltage V_o, seen by the tank, changes polarity with $i(t)$. Resonant capacitor voltage $v(t)$ is phase shifted with respect to $i(t)$ and peaks when $i(t) = 0$.

The input power from the positive half cycle is given by

$$P_{in} = \frac{V_{dc}}{T_3}\left[\int_0^{T_1} -i(t) + \int_{T_1}^{T_2} i(t)\right]$$

Normalising the above and substituting the current integrals and time interval notations given in fig. 3,

$$P_{in} = \frac{(-A_3 + A_1)}{\gamma} \quad (6)$$

Similarly, the output power can be written as

$$P_{out} = \frac{M(A_3 + A_1 + A_2)}{\gamma} \quad (7)$$

Equating (6) and (7) we get a relation for the voltage gain as

$$M = \frac{A_1 - A_3}{A_1 + A_2 + A_3} \quad (8)$$

For the PM-SRC, the load current is the rectified and filtered resonant tank current. That is, under steady state, the average of the rectified $i(t)$ over a cycle (or a half cycle) is the load current.

$$I_o = \frac{A_1 + A_2 + A_3}{\gamma}$$

The output voltage can now be related with a static load, R_{load}, and I_o as

$$V_o = I_o R_{load}$$

$$M = \frac{(A_1 + A_2 + A_3)}{Q\gamma} \text{ (normalised)} \quad (9)$$

Some conclusions can be drawn from relations (8) and (9). From (8) $M \leq 1$; the output voltage cannot be more than the input (without transformer/multipliers). On heavy loading ($R_{load} \cong 0$) M approaches zero. In such a case, $A_1 \cong A_3$; the energy input to the tank is returned to the source. The area A_1

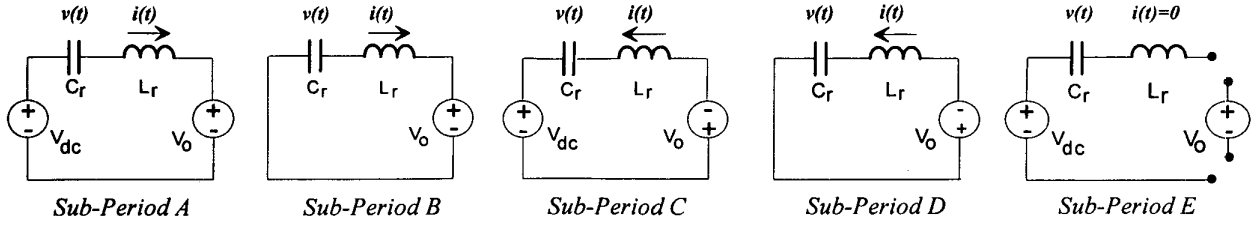

Fig. 2. Equivalent circuits of the different positive half sub-periods for the PM-SRC operating above resonant frequency.

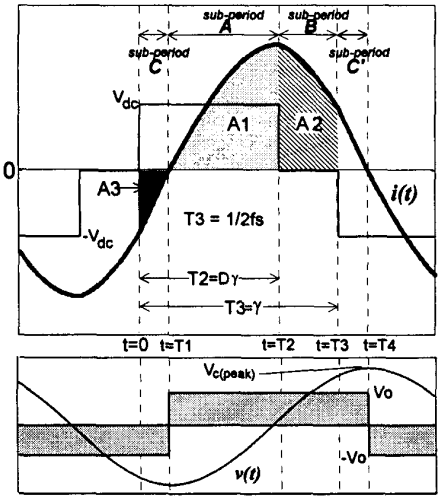

Fig. 3. MODE 1 operation waveforms

gives an indication of the amount of energy drawn from the source and the area A_3 indicates the amount of energy returned.

To determine A_1, A_2, A_3 and thus the voltage gain, equations for $i(t)$ in each of the sub-periods have to be evaluated. This is obtained by writing the circuit equations for the equivalent circuits of each sub-period (fig. 2) and substituting the initial conditions. Starting with *sub-period* A (fig. 3), the initial conditions for the equations in this sub-period are determined as $I(T_1) = 0$ and $V(T_1) = -V_{c\,(peak)}$ (negative peak voltage of C_r). The final conditions at the end of the *sub-period* A form the initial condition for the next sub-period. Equations for *sub-period* C are obtained by considering its final conditions (which are the initial conditions for *sub-period* A). The peak resonant capacitor voltage is given as

$$2V_{c\,(peak)} = \frac{1}{C_r}\left[\int_{T_1}^{T_2} i(t) + \int_{T_2}^{T_3} i(t) + \int_{T_3}^{T_4} i(t)\right]$$

$$V_{c\,(peak)} = \frac{A_1+A_2+A_3}{2} \text{ (normalised)} \qquad (10)$$

From (9) and (10)

$$V_{c\,(peak)} = \frac{MQ\gamma}{2} \qquad (11)$$

Equation (11) gives the peak resonant tank voltage stress for the circuit. For a given voltage gain and switching frequency, $V_{c\,(peak)}$ depends on Q. Thus the tank voltage stress will be more for a heavy load.

The equation for the voltage gain M is finally obtained in terms of γ, Q, D and the cross over time T_1. A second equation for T_1 is similarly obtained in terms of the other parameters. Both these equations are solved iteratively for different values of γ, Q and D to obtain M and T_1. The equations are valid for $0 < D < 1$, $f_s > f_r$ and $Q > 0$.

Time T_1 decides the mode boundary for MODE 1. The boundary condition being $0 < T_1 < D\gamma/2$. It can be seen that when $T_1 = 0$, $A_3 = 0$ and no energy is returned to the source. When $T_1 = D\gamma/2$, $A_1 = A_3$ and all the input energy is returned to the source (as in a dead short circuit).

The peak resonant tank (and the switch) current, rms and the average currents can be determined from the current equations. Both the legs of the inverter switches turn off with a positive current in MODE 1 operation. The tank current at $t = T_2$ and at $t = T_3$ are the turn off currents for the leading and lagging legs respectively. Equations obtained in the analysis are large in size and not suitable for manual calculation. A computer program in MATHCAD is used to solve them for different sets of values of γ, Q and D.

MODE 1 operation is a preferred operating region for the PM-SRC. Zero Voltage Turn on of all the four switches of the inverter is possible almost over the entire operating range of this mode. Turn off can be with low losses and device stress by using capacitive snubbers [1]. The tank current is continuous and nearly sinusoidal, eliminating stress on the output rectifiers. The disadvantages include large conduction losses due to the large peak currents and higher voltage stress.

F. Analysis of MODE *2 Operation*

MODE 2 consists of sub-periods A, B and D for half a cycle of operation. The cycle is defined to start at $t = 0$ with *sub-period* A followed by *sub-period* B. Tank current reverses direction at $t = T_2$ before the application of $-V_{dc}$, resulting in *sub-period* D. Fig. 4 gives the relevant plots for this mode.

Following the same procedure as for MODE 1 analysis, the equations for this mode of operation are derived and presented below.

$$M = \frac{A_1}{A_1+A_2+A_3} \qquad V_{c\,(peak)} = \frac{MQ\gamma}{2}$$

Here too, $M < 1$ over the entire mode of operation. The peak resonant capacitor voltage equation is same as that given by (11) for MODE 1 operation. The initial conditions for deriving the equations for the sub-periods are those at $t = T_2$; that is, $I(T_2) = 0$ and $V(T_2) = +V_{c\,(peak)}$.

As before, equations for the voltage gain and time T_2 are obtained and solved iteratively over the valid range of variables γ, Q and D. MODE 2 is bounded by MODE 1 and MODE 3. The boundary with MODE 1 is given by $T_2 < \gamma$. The

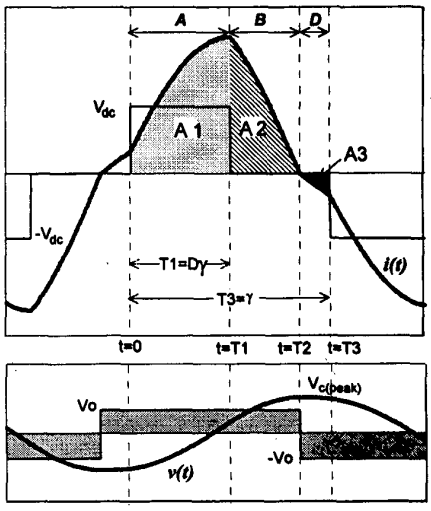

Fig. 4 PM-SRC waveforms for MODE 2 operation

other boundary is dictated by the γ and Q of the converter and is covered in the next subsection.

The leading and lagging leg turn off currents occur at $t = T_1$ and $t = T_3$ respectively. As is MODE 1 the analysis method returns large equations that need iterative calculations.

In this mode, the lagging leg switches turn off with a negative current. This means the diodes across the switch turning off starts conducting and remains on when the other switch in the same leg turns on. It necessitates the use of external fast recovery diodes across the lagging leg switches to prevent shoot through. Clearly, this mode of operation is not preferred. However, by suitable modifications to the PM-SRC this disadvantage can be eliminated..

G. Analysis of MODE *3 Operation*

MODE 3 operation is a discontinuous operating mode. Fig. gives the plots for a cycle of operation. Other than *sub-period* A and *sub-period* B, similar to those in the previous two modes, there exists *sub-period* E where no energy transfer takes place in either direction. Tank current $i(t) = 0$ and resonant capacitor voltage is held constant at its peak. Only the resulting equations and relevant conclusions are presented below.

$$M = \frac{A_1}{A_1 + A_2} \qquad V_{c\,(peak)} = \frac{MQ\gamma}{2}$$

$M < 1$ and $V_{c\,(peak)}$ has the same representation as before. Initial conditions at $t = 0$ are $I(0) = 0$ and $V(0) = -V_{c\,(peak)}$.

The boundary of MODE 3 with MODE 1 is given by $T_2 < \gamma$. Analysis of MODE 2 and MODE 3 data verifies that for a given γ and varying D, they never occur together for the same Q. Further, *sub-period* E of MODE 3 exists because $V(T2) = V_{c\,(peak)} < M$. Circuit analysis of *sub-period* E shows that this prevents $i(t)$ from changing direction at $t = T_2$. In case the capacitor voltage is higher than load voltage, $i(t)$ changes direction resulting in MODE 2. Therefore, for MODE 3 to exist

$$V_{c\,(peak)} < M \text{ or, } \frac{Q\gamma}{2} < 1 \qquad (12)$$

The leading leg switches turn off with a positive current while the lagging leg switches turn off with zero current (ZCS).

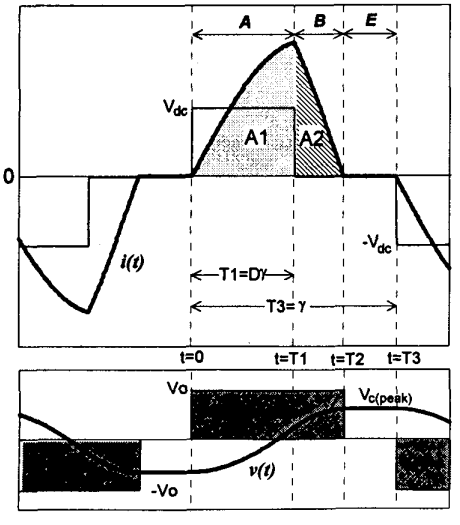

Fig. 5 MODE 3 operation waveforms

MODE 3 operation is preferred [4] for its relatively low peak currents and ZCS features. The disadvantages include the low turn off current for the leading leg switches (preventing ZVS), complete loss of ZVS for the lagging leg switches, non-sinusoidal current and low power delivered.

IV Analysis Results

Equations from the preceding section for each mode are solved and combined to obtain graphs required for understanding the functioning and for the design of the converter. There are three independent variables namely, the ratio γ, converter load factor Q and the control parameter D, which decide the operating point for the converter. The other independent parameters are either assumed constant or taken care during the normalisation of the equations. In the results presented here, one of the three parameters is held constant in order to simplify the graphs.

A. Voltage Gain

Fig. 6 gives the voltage gain (M) versus the control parameter (D) for six different load conditions. The gain response is seen to be large for low loads. For higher loading, the voltage gain is lower and the response to changing D is small at higher duty ratio. The PM-SRC is suited for wide load ranges including no load .

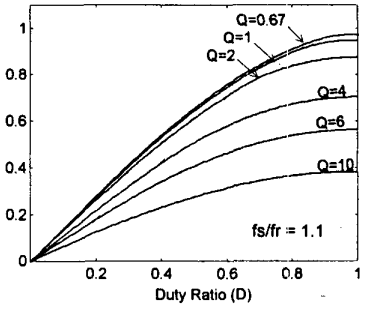

Fig. 6 Voltage Gain

B. Mode Boundaries

For $f_s/f_r = 1.1$, the operating modes are distributed as in fig. 7 for different load and duty ratio. The MODE 2 - MODE 3 boundary is a straight line given by (12). While MODE 1 operation is dominant for large Q , the light load conditions result in MODE 3 operation. For a fixed load the operating point may be chosen in MODE 1 or MODE 3. The thick line representing a voltage gain of 0.6 is seen to traverse through all the three modes for a varying load. Therefore the negative current turn off, characteristic to MODE 2, has to be taken care for such a varying load.

C. Output Power

Maximum power transfer occurs when the load impedance matches the resonant tank impedance. The effective impedance offered by the resonant tank depends on the tank elements and f_s. The resonant tank elements L_r and C_r, offer individual reactive impedance which cancel out at $f_s = f_r$. The value of this effective impedance increases as $(f_s - f_r)$ increases or as γ decreases. Consequently when the switching frequency is close to the resonant frequency, maximum power is delivered for high Q values and vice versa. Fig. 8 givens the output power versus load for $\frac{f_s}{f_r} = 1.1$. The maximum power output is obtained at around $Q = 4$.

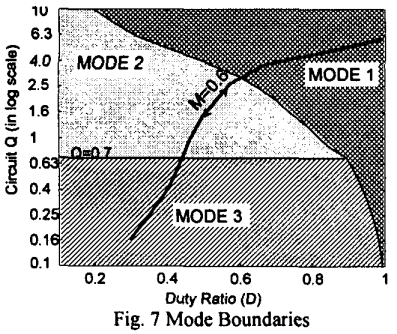

Fig. 7 Mode Boundaries

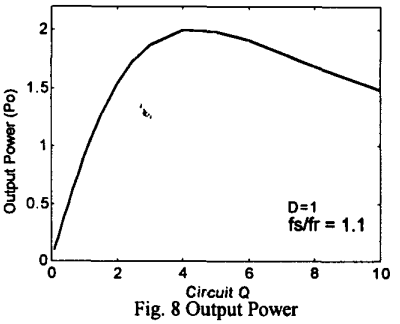

Fig. 8 Output Power

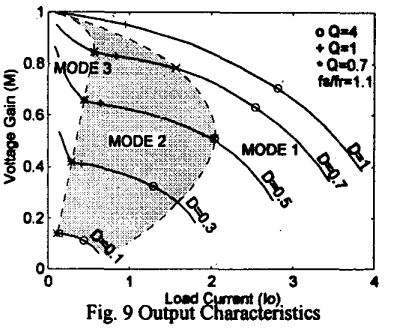

Fig. 9 Output Characteristics

D. Output Characteristics

Plots of output voltage versus the load current over a load range of $Q = 10$ to $Q = 0.1$ are given in fig. 9. Also marked are the zones for the different operating modes. MODE 2 is observed to show a nearly constant voltage characteristics while MODE 3 shows characteristics of a current source. The output current limiting property of the PM-SRC is evident here. For the switching frequency given, the output current is limited to about 4.3 units under short circuit.

Similar curves can be obtained for the peak electrical stress and switch turn off currents. In general, as f_s moves away from f_r, the electrical stress, power delivered and voltage gain decrease.

V MODIFIED SCHEMES

A. Extending ZVS Range

A varying load may push the operation of the PM-SRC into MODE 2 or MODE 3 (fig. 7). This results in not only loss of ZVS but heavy stress on the anti-parallel diodes of the MOSFET switches. [2] introduced a method of increasing ZVS range of phase modulated resonant transition converter by including an external inductive circuit. This method can be extended to the PM-SRC and the disadvantages of MODE 2 and MODE 3 operations can be eliminated. Fig. 10 gives the schematic. An external inductor L_{ex} is connected between node B of the lagging leg and node E. Node E is held at a stiff voltage $\frac{V_{dc}}{2}$ maintained by the large divider capacitors C_{ex1} and C_{ex2}. Since S_2 and $\overline{S_2}$ are complementary to each other, the voltage V_{EB} across L_{ex} will be a square wave switching between $\pm V_{dc}/2$ at the switching frequency of the converter (f_s). Sum of the external inductor current $iex(t)$ and the tank current $i(t)$ flows through the switches. The peak negative turn off current and the peak external inductor current ($I_{ex\,(peak)}$) coincide and by proper design, the net current flowing through the switches can be made non-negative. The design to restore ZVS would be; $I_{ex\,(peak)}$ = negative turn off current plus the current needed to discharge/charge the snubber capacitors across the switches. An expression for the value of the external inductor can be derived. Inclusion of L_{ex} does not effect the tank current and thus the analysis for the modified PM-SRC remains the same.

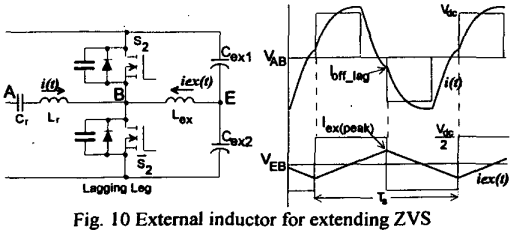

Fig. 10 External inductor for extending ZVS

B. Short Circuit Protection through Resonant Capacitor Clamping [5]

Short circuits on the load side in the form of arcing are common in high voltage power supplies. Even though the load current is limited on short circuits (fig. 9), there is an increase in the peak tank energy which leads to large tank current and voltage oscillations. An inherent short circuit protection method for the PM-SRC is used here. The tank energy is prevented from increasing beyond a predetermined limit by diverting the energy back to the source. This is achieved by clamping the resonant capacitor to a stiff voltage and preventing its voltage from building up to high values. The new method of clamping is given in fig. 11. It consists of a clamping transformer (X_{clamp}) with two secondary Sec_1 and Sec_2.The primary Pri is connected across C_r. Both the secondary windings are connected through fast diodes D_{clamp1} and D_{clamp2} to a common stiff voltage source which invariably is the dc supply voltage V_{dc}. Both the secondary are similar except for the winding polarity. The turns ratio, $Pri : Sec_1 : Sec_2 = N_{clamp} : 1 : 1$, decides the clamping voltage V_{clamp}. $V_{clamp} = N_{clamp} V_{dc}$, decides the maximum resonant tank voltage. Any increase of $v(t)$ beyond will activate the clamping diodes, sending back the tank energy.

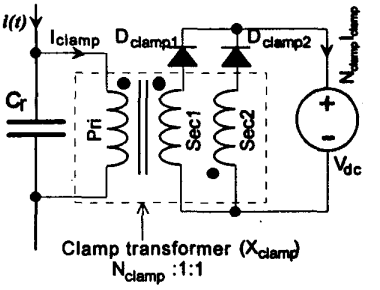

Fig. 11 The new resonant capacitor clamping method

In the present design, N_{clamp} is so chosen that the clamping occurs only above the maximum rated load. That is, if the converter is subject to overload, $v(t)$ will increase and C_r gets clamped to voltage V_{clamp}.

VI SIMULATION AND EXPERIMENTAL RESULTS

Results of the steady state analysis is verified using numerical simulation. These are further compared with the experimental results on a prototype converter. Parasitics were avoided in the numerical simulation model. Measurements for

the variable load were done without using the output transformer. The prototype specifications are as below:

$V_{dc} = 40V, f_s = 100kHz, P_o = 200W(average), f_s/f_r = 1.1$

$V_o = 1kV$ [25V without transformer], $Z_c = 11.6\Omega$

A. Voltage Gain

Table III compares the voltage gain (normalised) obtained from the analysis, simulation and as measured on the prototype for $f_s/f_r = 1.1$. Analysis and simulation results match very closely. If the output rectifier diode drop of 0.04 units is considered, the experimental results too match closely. Other parameters that effect the experimental data are the circuit parasitics like the switch conduction drop.

TABLE III VOLTAGE GAIN

Q	D	Analysis	Simulation	Measured
0.4	0.2	0.37	0.35	0.34
	0.5	0.72	0.73	0.69
	0.9	0.97	0.98	0.92
4	0.2	0.22	0.22	0.18
	0.5	0.51	0.51	0.47
	0.9	0.7	0.7	0.64

B Output Power

Since the voltage gain readings match closely, the power output will also be showing a similar trend. Fig. 12 plots the simulated and measured output power for a fixed duty ratio with $f_s/f_r = 1.1$. As predicted, maximum power is delivered at a Q of around four.

C. Output Characteristics.

Actual output characteristics given in fig. 13 show improved performance for overloads compared to the predicted curves of fig. 9 owing to the resonant capacitor clamping. The effect of clamping is further demonstrated in fig. 14. Tank current limiting for an output short is evident.

Fig. 15 shows the improvement in lagging leg switch dynamics on using the external inductor. Figs. 16-18 show the different modes of operation of the converter for different loading conditions.

VII CONCLUSION

The phase modulated series resonant converter is well suited for high voltage power supplies with variable load. Above resonant frequency operation facilitates ZVS for a MOSFET based converter. The preferred operating regions were found to be MODE 1 and MODE 3. However, using an external inductive circuit, the full operating range can be utilised. Inherent load current limiting capability makes it preferable. Additional inherent overload protection for the devices can be achieved by clamping the resonant capacitor voltage.

Experimental measurements on the scaled down model show good results verifying the design procedure.

VIII REFERENCES

[1] Robert L. Steigerwald, "A Comparison of Half-Bridge Resonant Converter Topologies," *IEEE Trans. Power Electronics*, vol. 3, No. 2, Apr. 1988, pp 174-182.

[2] Rajapandian A., "A Constant Frequency Resonant Transition Converter, " M.Sc. thesis, Dept. of EE, Indian Institute of Science, Aug. 1995.

[3] V. Vorperian, S. Cuk, "A Complete DC Analysis of the Series Resonant Converter," *IEEE Power Electronics Specialist Conf. 1982 Rec.*, pp 85-100

[4] Khai D. T. Ngo, "Analysis of a Series Resonant Converter Pulse Width Modulated of Current-Controlled for Low Switching Loss," *IEEE Trans. on Power Electronics*, vol 3, No.1, Jan 1988, pp. 55-63

[5] Biju S. Nathan, V. Ramanarayanan, "A New Resonant Capacitor Clamping Method for Series Resonant Converters, " *5th Brazilian Power Electronics Conf. COBEP'99*, Brazil, Sept. 1999.

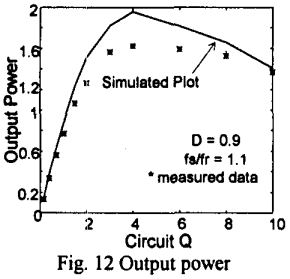

Fig. 12 Output power

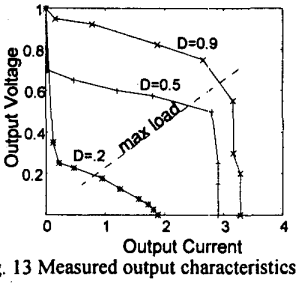

Fig. 13 Measured output characteristics

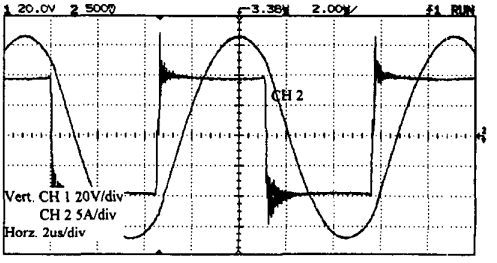

Fig. 14 Plot of tank current under a dead short circuit

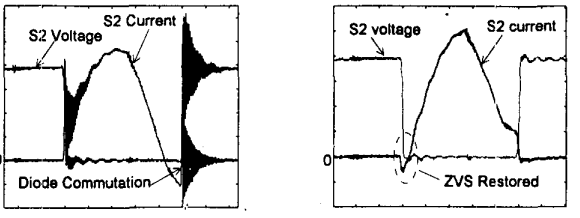

Fig. 15 Oscilloscope plot of lagging leg switch voltage and current without and with the external inductor.

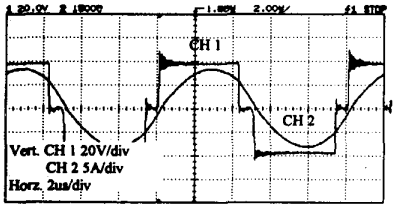

Fig. 16 Oscilloscope plot of MODE 1 operation

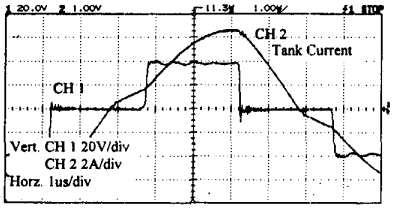

Fig. 17 Oscilloscope plot of MODE 2 operation

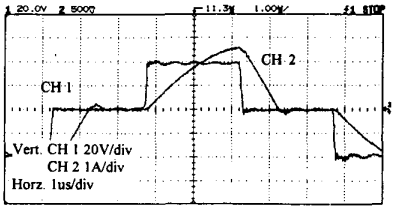

Fig. 18 Plot of MODE 3 operation